DISCRETE 3D MODEL OF MOLECULAR DIFFUSION THROUGH THE NUCLEAR PORE COMPLEX

A Thesis Submitted to the
Temple University Graduate Board

In Partial Fulfillment
of the Requirements for the Degree
MASTER OF SCIENCE

---

by
Star-Lena J. Quintana
July 2015

Thesis Approvals:

Isaac Klapper, Thesis Advisor, Mathematics
Weidong Yang, Biology
Wei-Shih Yang, Mathematics

ABSTRACT

Nuclear pore complexes (NPCs) are passageways that exist within the nuclear envelope (NE) of a eukaryotic cell. Molecular cargo travel through the passageways to either import to the nucleus or export to the cytoplasm of the cell. Efficient export of certain cargo is necessary for maintained health of a cell, and hence, the organism. Traditional methods of observing NPCs lack resolution great enough for scientists to study the many interactions that take place inside of the complex. A discrete 3D model of the molecular diffusion was built to understand how cargo moves through the NPCs and how to improve import and export efficiency of particular molecules. The basis of the model is a Langevin equation that was customized to the environment of the central channel of a NPC. The model incorporated not only the Brownian motion of the molecules, but also the geometry of the channel, the diffusion coefficient for molecules in the fluid of the central channel, and a potential energy (PE) function to describe drifting affects by the dense layers of phenylalanine-glycine (FG) repeats located in the channel and a concentration of transport receptors located on either ends of the NPC. The model simulated the movement of spherical molecules through the NPC and kept track of their location during their transport. The model showed that the cargo's movement has a distinct dependence on the PE function. The model can be further, and easily, manipulated and used for more comparisons to experimentally determined export efficiency for different cargo.

ACKNOWLEDGMENTS

First, I would like to express my gratitude to my advisor, Dr. Isaac Klapper, for his support throughout my time of research. He continuously pushed me to do my best so I could write a thesis that I would be proud to call mine. Without his patience and willingness to meet and discuss at any time, I cannot imagine that I would have completed my thesis in the timely manner that I did.

My gratitude also extends to the other members of my committee who, not knowing me as well as my advisor, still helped me along the way. I cannot thank Dr. Weidong Yang enough for his easy-to-comprehend explanation of the biological processes that I was modeling, nor Dr. Wei-Shih Yang for broadening my knowledge of various probability topics that was necessary for my model to be successful.

I would also like to thank the other professors in the mathematics department who gave me critical feedback on my thesis defense which, ultimately, made my thesis stronger. I am also grateful to my many colleagues who have helped me fix coding errors and gave me input throughout this journey; especially Fadoua who has repeatedly offered me a bed (and great tea) at her residence the many times commuting took its toll on me.

Most of all, I must thank my always supportive and encouraging fiancé and family. My fiancé, Eric, understood when I needed space to do a 12-hour writing session, but also made sure I did not forget to eat. I cannot thank him enough for loving me and taking care of me (especially by doing most of the chores during these last few months). My parents have always told me that getting an education is the most important thing to do in life because what you learn can never be taken away from you. Because my family has always believed in me, I have been able to continue my education and achieve this success. This degree is not just mine, but one for my whole family.

TABLE OF CONTENTS

LIST OF FIGURES

LIST OF TABLES

CHAPTER 1

INTRODUCTION

1.1 Nuclear Pore Complex

All of the cells that make up living beings can be classified into two groups: prokaryotic and eukaryotic cells. Eukaryotic cells differ from prokaryotic, or bacteria and archaea cells, by having membrane-bound organelles, notably cell nucleii [14]. Most of the cell's genetic material is housed in the nucleus, which is bounded by a double membrane, the nuclear envelope (NE) [25]. The NE separates the nucleus from the cytoplasm, which is the fluid that fills the cell [5]. However, because proteins and genetic materials need to move in and out of the nucleus, there are passageways along the NE, called nuclear pore complexes (NPCs), that allow diffusion and transport to occur [10].

Functioning NPCs are crucial in many aspects of cellular processes, since anything that requires transport between the nucleus and the cytoplasm will be affected by NPCs, the gated facilitators of molecular exchange between the two compartments [9]. Some examples of cellular physiology that require NPCs include regulation of gene expression, signaling, cell cycle control, and cell division [2]. In particular, RNAs that are synthesized in the nucleus have to be exported to the cytoplasm so they can aid in protein synthesis, and proteins needed for functions in the nucleus must be able to be imported efficiently from where they were synthesized in the cytoplasm [5].

NPCs are octogonally rotational symmetric structures [9] that contain three parts: the nuclear basket, the central channel, and the cytoplasm [22], see Figure 1. The nuclear basket is made up of filaments bound by a distal ring and is attached to the nuclear face of the NPC central channel [9]. The central channel is cylindrical and has eight spokes circling the region [22]. The cytoplasmic face is attached to filaments that act as docking site for transport receptors called karyopherins (kaps). Approximately thirty nucleoporins

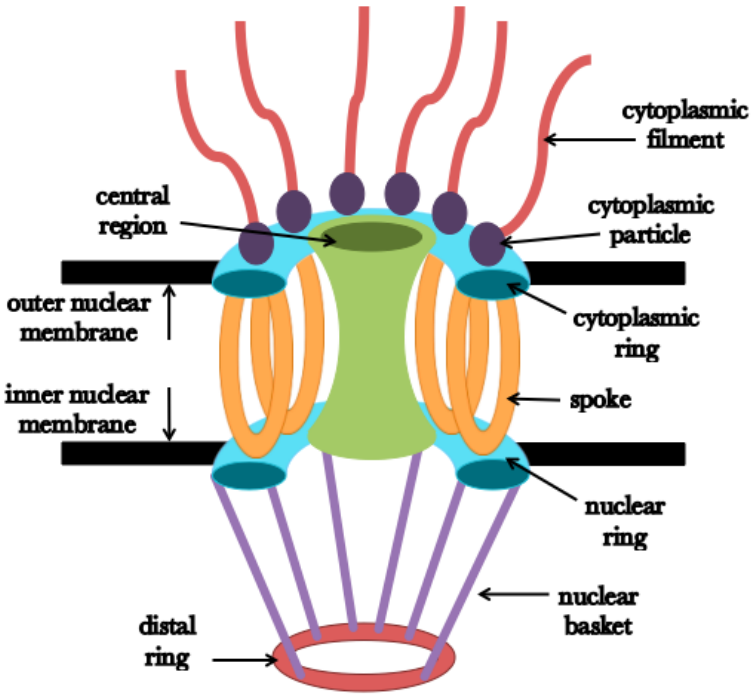

Figure 1: 3D model of the nuclear pore complex, which has an assembly of eight spokes that attach the nuclear and cytoplasmic ends of the envelope. Inside of the assembly is a central channel where particles pass through. Adaptation from [22].

(Nups) make up NPCs and one-third of them contain phenylalanine-glycine (FG) repeats which create a diffusion barrier between the nuclear section and cytoplasm [9]. Molecules transporting from the nucleus to the cytoplasm will be referred to as "exporting," while molecules transporting from the cytoplasm to the nucleus will be referred to as "importing."

Molecules can diffuse through the NPC two ways: passive diffusion where molecules can move freely (e.g. ions, metabolites, small macromolecules and proteins less than 5-10 nm in diameter) or facilitated diffusion where molecules are too large to pass on their own (e.g. ribosomal subunits with diameter 25 nm and larger cargo up to 40 nm) [10]. Large molecules that need help getting through the permeability barrier use the transport receptors (kaps) that dock at the FG repeats [9]. Kaps, such as importin-β used for importing and crm1 used for exporting, will have to interact with the FG repeats during transport. When large particles import to the nucleus, they will first bind to importin-β to form a protein complex and then travel through the NPC. Once the complex reaches the nuclear side, it

will then bind to another protein, Ran-GTP, that is located in the nucleus which will cause the protein complex to decompose so that the importin-β can go back to the cytoplasm and the traveling molecule will import to the nucleus. Guanine nucleotide-binding proteins, or G proteins, go through a hydrolysis where they bind to guanosine triphosphate (GTP) and are considered to be active and will transmit signals or bind to guanosine diphosphate (GDP) and are considered inactive. In the NPC, a G protein Ran can bind to GTP on the nuclear side and GDP on the cytoplasmic side. The GTP acts as a source of binding energy for the protein that is transporting through the NPC with the help of the transport receptor. Binding energy is generated in the nucleus so there is a high concentration of GTP in the nucleus. After proteins are transported through the NPC, GDP is the product of GTP so there is a high concentration of GDP in the cytoplasm from proteins being exported with the help of GTP. A similar process occurs when large molecules export from the nucleus: a protein complex is formed with crm1 and then Ran-GDP from the cytoplasm decomposes the complex to allow the molecule to exit into the cytoplasm.

The binding energy between a molecule and a transport receptor interaction is still unknown, however, as in [4], it can be described by the change in enthalpy, ΔH, which can be approximated by the Coulombic interaction between the transport receptor and NPC and be given in units kT:

$$\Delta H \approx \frac{Q_{TR}Q_{NPC}}{\varepsilon \cdot l} = 55.3\frac{Q_{TR}Q_{NPC}}{\varepsilon \cdot l}kT \tag{1}$$

where Q_{TR} is the charge from the transport receptor, Q_{NPC} is the charge from the NPC, ε is the dielectric constant of water, and l is that distance between the transport receptor and the NPC (assumed to be 1 nm). In the second expression, Q_{TR} and Q_{NPC} are expressed in elementary charge units. In humans, $-120e \leq Q_{TR} \leq -20e$, where e is the electron charge [4]. Following the method outlined in [4], we can approximate this binding energy. Using the parabolic profile that describes the dimensions of the channel, the volume of the channel is 311016 nm^3. From [9], we have the approximation that there are about 30 nucleoporins present in the pore (with at least 8 copies each), so to conservatively estimate the average

number of nucleoporins within a hemisphere of radius 1 nm, we calculate $\frac{8 \cdot 30}{311016\text{nm}^3} \cdot \frac{2}{3}\pi \cdot 1$ $\text{nm}^3 \approx 0.0016$. The charge of a nucleoporin ranges, but we can approximate it be about $15e$ so that $Q_{NPC} \sim 0.0016 \cdot 15e = 0.024e$. With $\varepsilon = 80$, Equation (1) becomes

$$\Delta H \approx 0.017 \frac{Q_{TR}}{e}\, kT \tag{2}$$

If a transport receptor has a negative charge of $Q_{TR} = -50e$, the energy gain from the interaction is $\Delta H \sim -0.85$ kT.

Findings from [4] suggest that transport efficiency can be increased depending on the magnitude of ΔH, which is proportional to the change in potential energy. Since the NPC is positively charged, the interactions it has with negatively charged transport receptors may provide the binding energy needed to facilitate diffusion. However, it is believed that hydrophobic interactions between the transport receptors and the FG filaments are a driving force for transport [21] and the previously described static-electronic interactions play more minor roles.

While mechanistic and kinetic views on transport through the NPC still vary, there are three prominent models that aim to describe the hydrophobic interactions between the kaps and FG repeats: the selective phase model that says filaments form a meshwork that only kaps can dissolve through; the polymer brush model that says filaments exclude specific cargoes and promote access for kaps by collapsing; and the trees and brushes model that says there is a set distribution of extended and collapsed filaments that make distinct routes for kap-cargo complexes to diffuse through [21]. While binding activity cannot solely be described by the hydrophobic interactions the transport receptors have with the FG filaments, there is a distinct connection. Transport receptors bind strongly to the FG filaments near the pore walls and weakly to the extended filaments closer to the center of the pore. When the pore is crowded with extended filaments, the weak binding activity encourages faster transport of kap-cargo complexes to occur [21].

Throughout this paper, the proteins and other genetic material that transport through the NPC will be referred to as "particles." Of interest is the import and export efficiency of particles in the NPC. For example, if 100 particles attempt to export from the nucleus to the cytoplasm, and 50 of the particles successfully end up in the cytoplasm, the export efficiency is 50%. We will explore different scenarios that mimic different molecules and kap-cargo complexes transporting through the NPC.

1.2 Motivation

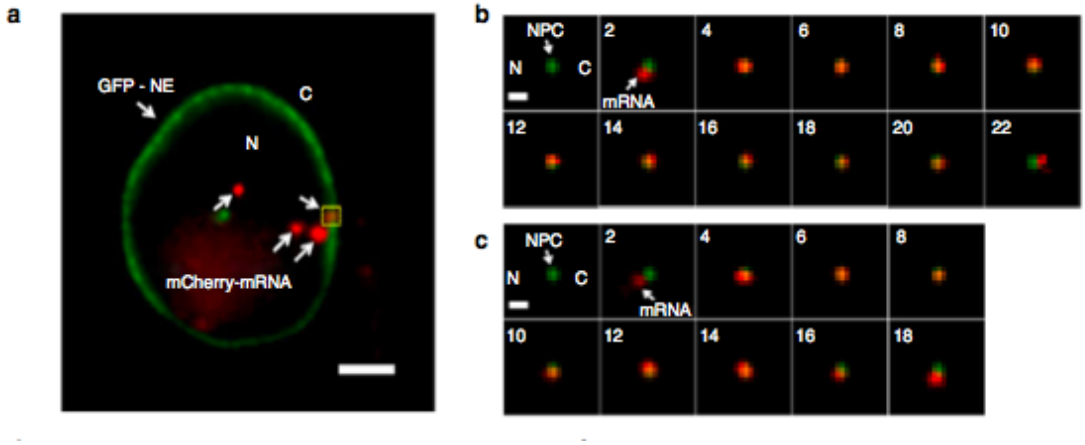

Figure 2: (a) Molecules (mCherry-mRNAs) inside of the nucleus (b) Successful export movement from the nucleus to the cytoplasm (c) Abortive event where the mRNA retreated back to the nucleus instead of exporting to the cytoplasm [11].

We have been working closely with Weidong Yang and his lab at Temple University, who have tracked the movement of particles through the NPC to try to better understand what factors influence their success or failure of importing and exporting. As shown in the data in Table (1), the export efficiencies of smaller particles such as messenger RNAs (mRNAs) seem to be around 50%. Additional (unpublished) data suggests that the export efficiencies of pre-ribosomal subunits and other large particles that interact with the NPC may be larger than 60%. A prominent theory for the cause of this increase in efficiency is that kaps aid facilitation. Yang and his team did further experiments to delve into the cause of increased efficiency by using various species of kaps. Their results show that multiple

Molecular name	Estimated diameter (nm)	Export efficiency
EGFP	4.49	$47 \pm 5\%$
Tap-p15	6.15	$54 \pm 5\%$
hCRM1	6.74	$53 \pm 5\%$

Table 1: Export efficiencies found experimentally [11]

kaps, when used together, increase the export efficiency of larger particles through the NPC. If the results could be validated mathematically, it would provide new insight to the energetics and mechanisms of the NPC. A 3D mathematical model of the nuclear pore complex could verify these and other experiments that try to show why some molecules have a higher export efficiency than others. Questions we would like to answer include: (1) What factors influence the success and/or failure of transport, and (2) what effects cause a change in transport efficiency? Knowing the requirements for efficient import and export can aid in maintaining the health of a cell by understanding how to retain certain molecules in the nucleus or release others to the cytoplasm.

1.3 Mathematical Background

1.3.1 Langevin equation

In literature, it is common to have the diffusion setting of the NPC be modeled by random walks [15]. For particles moving in a fluid, such as cytoplasm, collisions with the fluid molecules have two effects: induction of apparent Brownian force of the particle and generation of a frictional force that opposes motion induced by some external force [2]. Brownian motion, named for the botanist Robert Brown who observed pollen particles moving in water [3], is the random motion of particles suspended in a fluid [20].

The Langevin equation is a first order differential equation that describes the effects on a particle by the molecular collisions of the surrounding fluid [2]. In simplest terms, the equation is Newton's law of motion applied to a particle [6]. To arrive at the equation, the dynamics of a Brownian particle must first be outlined [13].

The Brownian particle's dynamics can be described by

$$\frac{dX}{dt} = V \tag{3}$$

$$m\frac{dV}{dt} = F \tag{4}$$

where m is the particle's mass, $X = X(x,y,z,t)$, $V = V(x,y,z,t)$ are the particle's position and velocity at time t, and F is the force acting on the particle by the molecules of the surrounding fluid. The force F consists of two parts, the first being the frictional force acting on the particle, which is proportional to the velocity [20]. The second part of the force is a random, or Brownian, force due to the collisions with the fluid's molecules. By the Central Limit Theorem [22], if we are looking at the forces over a long period of time, as we are, we can assume that the dynamics of these forces are Gaussian white noise [18]. Equation (4) can then be rewritten as

$$m\frac{dV}{dt} = -\zeta V + f_B(t) \tag{5}$$

where ζ is the frictional drag coefficient, such that $\zeta = 6\pi\eta R$ for a spherical particle that satisfies Stokes Law [1]. Equation (5) is the "classical" Langevin equation, which will be modified for our simulation.

1.3.2 Gaussian white noise

Noise is a stochastic, or random, process where a family of random variables indexed by time represents a system evolving over time. From communications theory, we have that the property of "whiteness" means that the random variables are independent, where here, independent means that for each time, the distribution of the future random variables does not depend on the outcomes of the present and past random variables. "Gaussian" refers to variables that are normally distributed with a zero mean and finite variance. For discrete

time cases, the variance is $\frac{1}{\Delta t}$, where Δt is the length of time interval. The random variables multiplied by Δt are normally distributed with mean zero and variance Δt. For the continuous case, since Δt goes to zero, the limiting family does not exist as Gaussian distributions. However, when the random variables are integrated over an arbitrary interval length, I, with respect to time, the distribution is normal with mean zero and variance I. In the context of transport in the NPC, the random forces acting on the particle from colliding with the molecules of the fluid will be described by a Gaussian white noise distribution because of the Central Limit Theorem which states that when a sample size is large enough (in our case, the number of collisions), the distribution will be (or close to) normal with respect to space [17]. For our purposes, the white noise will be integrated, and we see from Equation (5) that when this happens, the integration will yield a Gaussian distribution which will describe the distance that the particle is displaced due to the Brownian, or random, forces.

1.3.3 Mean square displacement of particles

Without solving the diffusion equation (6), where $\rho(x,t)$ is the particle density at position x and D is the diffusion coefficient, we can find a relationship between the Brownian motion of the particles and their diffusion [7]. We are able to do this because the Brownian motion that the particles encounter on the microscopic scale of the collisions with the fluid's molecules ultimately lead to the particle's diffusion on a larger scale.

$$\frac{\partial}{\partial t}\rho(x,t) = D\frac{\partial^2}{\partial x^2}\rho(x,t) \tag{6}$$

Since the probability, P, of a particle being at x is proportional to the particle density at x, we can use the probability distribution to describe the particle's movement.

$$\rho(x,t) \propto P(x,t) \tag{7}$$

By studying the particle's random and irregular trajectory, we can find the average quadratic displacement (also called the mean square displacement: a way of measuring the magnitude of movement in terms of distance) of the particle. For one dimension (x), the probability that a particle's displacement is between x and $x+dx$ after t seconds is defined to be $P(x,t)dx$ where we have the normalization

$$\int P(x,t)dx = 1. \tag{8}$$

The average displacement for a large number of particles is defined by

$$< x >= \int xP(x,t)dx = 0 \tag{9}$$

The average displacement is zero due to the assumption of no external forces acting on the particle so that both positive and negative displacements occur with equal probability. Now, the average quadratic displacement is found by integration

$$< x^2 >= \int x^2 P(x,t)dx \tag{10}$$

We want to see how the MSD changes over time by looking at the diffusive time scale.

$$\begin{aligned} \frac{d}{dt} < x^2 > &= \int \frac{\partial}{\partial t} x^2 P(x,t)dx \\ &= D \int \left[\frac{\partial}{\partial x^2} P(x,t) \right] x^2 dx \end{aligned} \tag{11}$$

Under the assumption that $P(x,t)$ and its derivative monotonically decrease to 0 for x going to infinity, integration by parts on (11) gives

$$\begin{aligned} &\frac{d}{dt} < x^2 > = 2D \\ &\Rightarrow < x^2 > = 2Dt \text{ for } \tau << t, \end{aligned} \tag{12}$$

which gives the relation between the Brownian motion and diffusion. The above process is identical for other directions y and z [1]; therefore, the MSD of a particle diffusing in any direction $\overrightarrow{r}$ is

$$< r^2 > = < x^2 > + < y^2 > + < z^2 > = \ 6Dt. \tag{13}$$

The MSD of particles is also found by looking at the changes in distance for a particle on a diffusive time interval (time it takes for particles to diffuse a small distance). In one dimension (x), a particle with mass m and velocity v has a kinetic energy of $KE = \frac{1}{2}mv^2$. On average, however, a particle at absolute temperature T has a kinetic energy of $< KE >$ $= \frac{k_B T}{2}$, regardless of particle size, where the $<$ and $>$ brackets denotes averaging and k_B is Boltzmann's constant [1]. Together,

$$\begin{aligned} < \frac{1}{2}mv^2 > &= \frac{k_B T}{2} \\ < v^2 > &= \frac{k_B T}{m} \end{aligned} \tag{14}$$

If we look at Brownian dynamics on a diffusive time scale , $\tau << t$, for a large number of steps $n = \frac{t}{\tau} >> 1$, we can calculate

$$\begin{aligned} < x^2 > \sim n < v^2 > \tau^2 &= \frac{t}{\tau}\frac{k_B T}{m}\tau^2 \\ &\sim t\tau\frac{k_B T}{m} \\ &\sim \frac{k_B T t}{C} \end{aligned} \tag{15}$$

where C is some proportionality constant.

After comparing the two results (12) and (15), we see that that D is proportional to $\frac{k_B T}{C}$. This results in the Einstein-Smoluchowski relation, $D = \mu k_B T$, where μ is the mobility coefficient of particles (which, in the limit of a low Reynolds number–a dimensionless number that measures the ratio of inertial forces to viscous forces–is $\mu = \frac{1}{\zeta}$) [16]. Throughout this paper, we will use $D = \frac{k_B T}{\zeta}$ as the Einstein-Smoluchowski relation.

CHAPTER 2

LANGEVIN MODEL

In order to study the efficiency of particle transportation through the NPC, a 3D simulation of a spherical particle moving through the central channel of the NPC was created using MATLAB. For the simulation, the diffusion was modeled by a modified version of the "classical" Langevin equation. Due to the molecular scale of these particles and the high viscosity that is present in the NPC environment, the Reynolds number is very small. The small Reynolds number allows us to assume the inertial term (i.e., acceleration term) of (5) to be negligible (see [16] for a more in-depth explanation). The particles are also acted on by external forces, which are characterized by a PE function. This PE mimics the setting of the asymmetric nucleoporins and FG repeats throughout the NPC that dictate the directionality of the particle's movement along with a high or low concentration of kaps at either end of the NPC. The PE is not dependent upon the path that the particle takes, but instead on its current position in the NPC. Using those two assumptions and the Einstein-Smoluchowski relation, we arrive at

$$\zeta \frac{dX}{dt} = f_B(t) - \nabla U \tag{16}$$

where $U = U(x,y,z)$ is the PE at the particle's current position. This can then be solved explicitly forward in time for the particle's position X. Inside the central channel of the NPC, $D = 0.07\frac{\mu m^2}{s}$ [11]. When provided D, we can rearrange the Einstein-Smoluchowski relation to find $\zeta = \frac{k_B T}{D}$. Assuming room temperature of $293K$, ζ is calculated to be $5.77 \cdot 10^{-8}\frac{kg}{s}$.

In order to see the displacement of the particle at each step, integration of Equation (16)

over a time variable, τ, gives

$$X(t+\Delta t) = X(t) + \frac{1}{\zeta}\left(\int_t^{t+\Delta t} -\nabla U(\tau)d\tau + \int_t^{t+\Delta t} f_B(\tau)d\tau\right) \tag{17}$$

$$X(t+\Delta t) \approx X(t) + \frac{1}{\zeta}\left(-\nabla U(t)\Delta t + \int_t^{t+\Delta t} f_B(\tau)d\tau\right) \tag{18}$$

where the last term, $\int_t^{t+\Delta t} f_B(\tau)d\tau$, is the Brownian motion displacement for each time interval (which is independent of each interval). Since f_B is a Gaussian white noise term, the integration of it will provide Brownian motion, a Gaussian normal distribution with mean 0 and variance $6D\Delta t$ (see sections 1.3.2 and 1.3.3) that describes the displacement of the particle for each time interval [18]. Clearly, we see that the particle's displacement will be affected by two forces, external and Brownian.

2.1 Initial set-up of the NPC

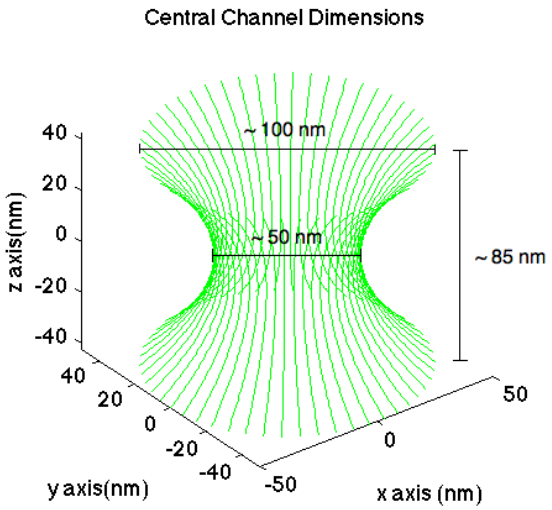

Figure 3: Illustration of the central channel of the NPC. The length from the nucleus ($-z$ end) to the cytoplasmic face ($+z$ end) is $\sim$ 85 nm; the outer width on each end is $\sim$ 100 nm; the center radius of the central channel is $\sim$ 50 nm. [24]

A discrete cylinder (Figure 3) was created to model the channel. The curvature and size of the cylinder was made using dimensions found in literature (see Table 2). The curvature

Parameter	Value	Units	Reference
k_B	1.38x10^{-5}	kg nm^2 s^{-2} K^{-1}	[8]
T	293	K	Assumption
D	7 x 10^4	nm^2 s^{-1}	[11]
ζ	5.8 x 10^{-8}	kg s^{-1}	Calculated
Channel Center Diameter	50	nm	[24]
Channel Outer Diameter	100	nm	[24]
Length of Channel	85	nm	[24]
Particle Diameter	6.25	nm	[12]

Table 2: Parameter values

and dimensions of the channel can be easily altered in the curve function file that is separate from the main script. After beginning at an initial position, the particle will randomly move throughout the NPC, dictated by (18). Physically, the particles cannot pass through the walls of the central channel. In the simulation, the cylinder will also forbid particles from passing through. The function, *curve.m*, that describes the curve of the cylinder can be called as follows

```
[Radius,r]=curve(zs); % curve: radius of the cylinder at z's
```

The function will input the z values of the cylinder and then output the the distance the edge of the cylinder is from the z-axis (*Radius*) and also the particle radius (r) (which is defined by the user). The actual file looks like

```
function [Radius, pr]=curve(zs)
% This function sets up the curve profile of the cylinder for
% all of the z coordinates once the user defines the center
% and outer diameter of the channel. It will also output the
% particle radius, which is defined by the user.
% -------------- User input ----------------%
center_diameter=50; % nm
outer_diameter=100; % nm
```

```
particle_diameter = center_diameter/8;   % nm
% ----------------------------------------%
cr=center_diameter/2;    % center radius
or=outer_diameter/2;     % outer radius
pr=particle_diameter/2; % radius of the particle
pb=(or-cr)/(zs(1)^2);    % parabolic constant describing the curve
Radius=pb*zs.^2 +cr;     % curve profile
```

2.2 Calculating the displacement

2.2.1 External force contribution

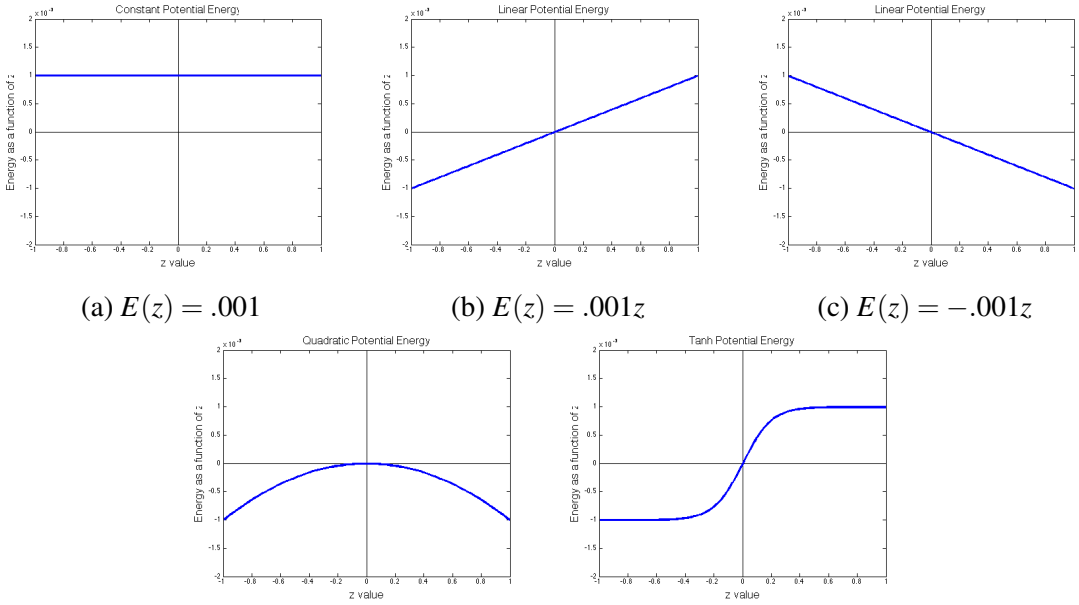

(a) $E(z) = .001$ (b) $E(z) = .001z$ (c) $E(z) = -.001z$

(d) $E(z) = -.001z^2$ (e) $E(z) = .001 \tanh 5z$

Figure 4: Potential Energy Functions: E [k_BT]

A PE function describes the energy of a particle, which in the case of these simulations, results from the particle's position. This PE is used to mimic how the makeup and location of the FG repeats and concentration of kaps affect the particle's movement. If there is available importin-β in the nucleus and crm1 in the cytoplasm, then the particle will be able to import or export. The gradient of the PE at the particle's location is found and is then used

to "drift" the particle. Five different PE functions were used in the simulation (Figure 4): a constant energy, positive and negative linear energy, quadratic energy, and hyperbolic tangent energy function. These different potential energy functions mimic cases that describe various concentration levels of kaps and particle size. A constant potential energy function was used to mimic the case when particles are small enough to passively diffuse through the NPC without interaction of the FG repeats or the kaps. Since the size of the particle is proportional to the available receptors at either end of the NPC, a linear energy function was used to incorporate effects of having particular kaps. Different magnitudes of slope can be varied to compare larger particles (large magnitude) and smaller particles (small magnitude). On the nuclear side of the NPC, we wanted to force the particles back into the nucleus, and on the cytoplasmic side, back into the cytoplasm. A negative quadratic energy function seemed to be a good model for this situation because it is a smoothed-version of a positively-sloped line joined with a negatively-sloped line. Another scenario of transport was modeled using an hyperbolic tangent energy function. Properties of this function are similar to the positive linear function where particles imported to the nucleus. However, by having a"flattened" level on the cytoplasm side, this is comparable to having a level of Ran-GDP on the cytoplasm side of the NPC that should help the particles export if they are close enough to the cytoplasmic face. Various energy functions can be used in this model; however, for simplicity and easy interpretation, these five were chosen to display the success of this model.

The units for PE in the simulation are kg nm^2 s^{-2}. We can convert this to units of kT in order to compare the PE to the binding energies discussed in 1.1. From Table (2):

$$1\text{kT} = 1.38 \cdot 10^{-5}\ \text{kg}\ \ \text{nm}^2\text{s}^{-2}\ \text{K}^{-1} \cdot 293\ \text{K} = 0.004\ \text{kg}\ \text{nm}^2\ \text{s}^{-2} \tag{19}$$

In our constant PE function, the energy is 0.001 kg nm^2 s^{-2}, which is $\sim$ 0.247 kT. This tells us that for all of the other functions, the PE ranges from -0.247 kT to 0.247 kT.

An example of how an energy function will need to be called within the main script is shown below, where the input arguments are the particle's current position and the radius of the particle.

```
1 drift=energy_linear_neg(current_pos,r);
```

Below is an example of an energy function file, *energy_linear_neg.m*, where line 8 is the equation of the PE. The user may write any necessary parameters before finding the gradient of the energy function (lines 4-6).

```
1  function drift=energy_linear_neg(center,r)
2  % This function will use symbolic tools to find the energy
3  % at the current position and output its gradient.
4  % ---- User Parameters --- %
5  alpha= .001;
6  %--------------------------%
7  syms x y z          % initializing symbols
8  U = -alpha*z;             % input function here using x, y, z
9  gradientofU = gradient(U, [x, y, z]); % solve for gradient of function
10 drift= double(subs(gradientofU,[x y z],center))'; % grad. at position
```

2.2.2 Brownian force contribution

Since the Brownian motion of the particle is described by a normal distribution, some numerical problems can arise when choosing a displacement amount, such as choosing an amount that dominates the external force and drastically changes the position of the particle. Instead of describing the movement by a Gaussian distribution, we will fix the displacement, which is possible by the Central Limit Theorem.

To begin, the change will be described in one dimension. In the x-direction, we have a

discrete random variable $x_i,\ 1 \leq i \leq n$ such that $x_1 + x_2 + ... + x_n \sim N(0, 2D\Delta t)$ (see 1.3.3). Instead, we will choose a Bernoulli variable, $y_i,\ 1 \leq i \leq n$ such that

$$y_i = \begin{cases} a & p = 0.5 \\ -a & q = 1 - p = 0.5 \end{cases} \tag{20}$$

In words, there is a displacement of $+a$ with probability $p = 0.5$, and a displacement of $-a$ with probability of $q = 0.5$. The expected value of this distribution is $E[y] = 0$ and the variance is $E[y^2] = a^2(0.5) + (-a)^2(0.5) = a^2$. If $a = \sqrt{2D\Delta t}$, then by the Central Limit Theorem [17], we have that $\frac{y_1+y_2+...+y_n}{\sqrt{2D\Delta t n}} \to N(0,1)$, which then implies that $y_1 + y_2 + ... + y_n \sim N(0, 2nD\Delta t)$. The desired Brownian displacement in the x direction can then be approximated by the Bernoulli random variable

$$y_i = \begin{cases} \sqrt{2D\Delta t} & p = 0.5 \\ -\sqrt{2D\Delta t} & q = 0.5 \end{cases} \tag{21}$$

This tells us that the magnitude of the Brownian displacement in one direction with our new variable is $\sqrt{2D\Delta t}$.

We saw in section 1.3.3 that the magnitude of the particle's spatial movement can be described by the MSD. It turned out that in one dimension, the MSD was $2D\Delta t$, and for 3 dimensions was $6D\Delta t$. In a similar manner, the approximate magnitude of displacement for the particle in 1D was found to be $\sqrt{2D\Delta t}$, and for 3D is then $\sqrt{6D\Delta t}$. The random 3D direction that the particle will move in due to the Brownian force will be determined by a uniform distribution of points on a spherical surface (see section 2.2.3).

In our case, the diffusion coefficient was assumed to be constant. However, because of the set up of the script, the user can change the diffusion to be spatial dependent if he/she chooses. The diffusion for the particle's current position is called by

```
1 D=diffusion_coefficient(current_pos);
```

The function file is written as the following

```
1  function D=diffusion_coefficient(current_pos)
2  % This function calculates the diffusion coefficient depending
3  % on the particle's current position.
4  % ----- User input ------------- %
5  Diffusion=70000;    % constant diffusion coefficient [nm^2/s]
6  % ------------------------------ %
7  x=center(1);
8  y=center(2);
9  z=center(3);
10 D=0*x+0*y+0*z+Diffusion;
```

where line 10 can be altered to be any relation the user desires.

2.2.3 Uniformly choosing points on a spherical surface

Since we were able to find a magnitude of the Brownian displacement, we now need to determine a way of choosing a random direction for the displacement. Since our model is in 3D, if we center a particle in an imaginary sphere, a vector from its position to each point on the surface of the sphere represents all of the possible directions the particle can move. We want the particle to have an equal chance of moving in all of those directions, so we need a way of uniformly distributing points on the surface of the sphere. We can do this by assigning probabilities for choosing a point in a segment of the surface of the sphere. The segment of the surface will then be defined by the azimuth (ϕ) and polar (θ) angles. We will need the surface area of the section to find the probabilities of generating a point in that section, which we can derive from the area element of the surface of revolution that

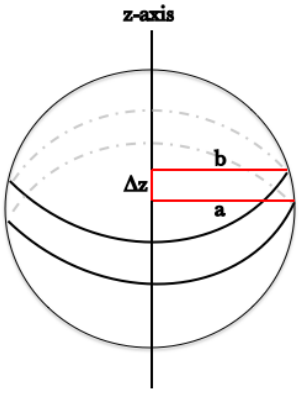

Figure 5: Segment of the spherical surface of revolution

stems from rotating a curve $x = f(z)$ from $z = a$ to $z = b$ about the z-axis

$$\begin{aligned} dS_z &= 2\pi x ds \\ &= 2\pi x\sqrt{1+(x')^2}dz \end{aligned} \tag{22}$$

where dS_z is the area element and s represents the x-z coordinates we are interested in such that $ds = \sqrt{1+(x')^2}dz$. The area element is such that the surface area of the sphere can be computed by

$$S = 2\pi \int_a^b x\sqrt{1+(x')^2}dz \tag{23}$$

where a is the lower radii of the segment, b is the upper radii of the segment (see Figure 5). In the x-z plane, $x = \sqrt{R^2 - z^2}$ describes a circle where R is the radius of the sphere. Then, $(x')^2 = \frac{z^2}{R^2-z^2}$ which will give us

$$
\begin{aligned}
S &= 2\pi \int_{\sqrt{R^2-a^2}}^{\sqrt{R^2-b^2}} \sqrt{R^2-z^2}\sqrt{1+\frac{z^2}{R^2-z^2}}dz \\
&= 2\pi R \int_{\sqrt{R^2-a^2}}^{\sqrt{R^2-b^2}} dz \\
&= 2\pi R\left[\sqrt{R^2-a^2}-\sqrt{R^2-b^2}\right] \\
&= 2\pi R\left[x|_b - x|_a\right] \\
&= 2\pi R\Delta z
\end{aligned}
\tag{24}
$$

only depends on the radius of the sphere R, and the height of the segment, Δz. This is interesting to note because, since the surface area of the segment does not depend on the position of the segment, if the sphere is divided into equal sections of height Δz, all of the points in those sections will have an equal probability of being chosen since their surface areas will be equal.

Since the segment of the spherical surface is defined by its angles ϕ and θ , these angles will be functions of uniformly distributed variables, u and v. To find what $\phi(u)$ and $\theta(v)$ need to be, we can first consider the volume element of the sphere

$$dV = r^2 \cos\phi \, dr d\theta d\phi \tag{25}$$

Assuming a radius of 1,

$$dV = \cos\phi \, dr d\theta d\phi \tag{26}$$

We find ϕ by requiring

$$\cos\phi(u) d\phi(u) = a_1 du \tag{27}$$

where a_1 is a proportionality constant. Integration yields

$$\sin\phi(u) = a_1 u + b_1 \tag{28}$$

where b_1 is an integration constant. For a sphere, $-\frac{\pi}{2} \leq \phi \leq \frac{\pi}{2}$, so that $\phi(0) = -\frac{\pi}{2}$ and $\phi(1) = \frac{\pi}{2}$. Using this information, a_1 and b_1 are found to be 2 and -1, respectively, so that

$$\sin\phi(u) = 2u - 1. \tag{29}$$

$$\phi(u) = \sin^{-1}(2u - 1). \tag{30}$$

The inverse sine in the ϕ expression takes care of the fact that we need fewer samples near the poles; otherwise, if a uniform distribution was chosen independently for each direction x, y, z, the distribution would "clump" near the poles of the sphere.

We can follow a similar method to find an expression for θ

$$d\theta(v) = a_2 dv \tag{31}$$

where a_2 is a proportionality constant. Integration yields

$$\theta(v) = a_2 v + b_2 \tag{32}$$

For a sphere, $0 \leq \theta \leq 2\pi$, so that $\theta(0) = 0$ and $\theta(1) = 2\pi$. Using this information, a_2 and b_2 are found to be 2π and 0, respectively, so that:

$$\theta(v) = 2\pi v \tag{33}$$

Now that we have expressions for the angles that define the segment of the sphere in terms of uniformly distributed variables, we can use MATLAB's *sph2cart* function to translate them into Cartesian coordinates. These coordinates then dictate a 3 dimensional direction for the Brownian displacement (see Figure 6).

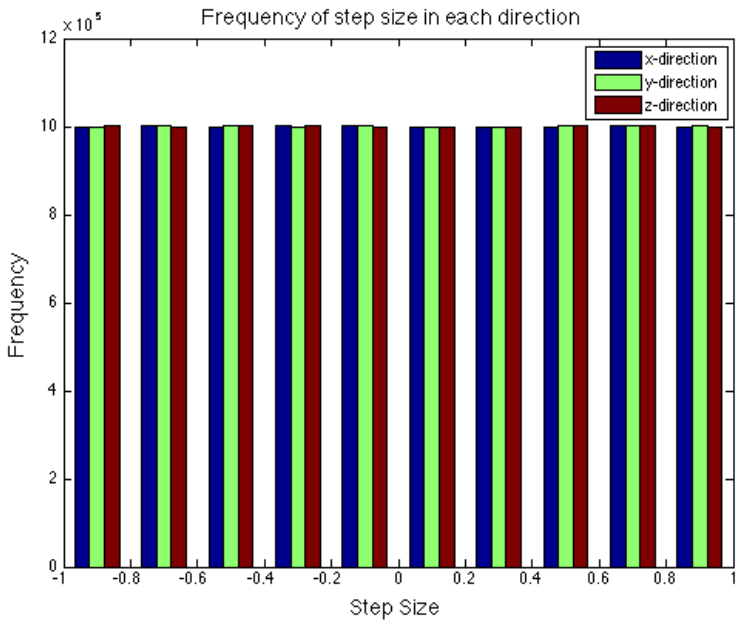

Figure 6: Using expressions (30) and (33), 10^6 samples of ϕ and θ were generated. MATLAB's *sph2cart* function was used to translate the variables into Cartesian coordinates. The histogram shows a uniform distribution of chosen step sizes for each x, y, and z directions.

2.2.4 MATLAB script

The following is a sample of the main script (which does not need to be edited by the user) that calculates the diffusion of the particle through the central channel.

```
D=diffusion_coefficient(current_pos); % Find D current position
zeta=kB*Temp/D; % friction drag coefficient [kg/s]
%-------------------------------------------------------%
% Find PE at current position to dictate drift
drift=energy_linear_neg(current_pos,r);
%-------------------------------------------------------%
% Uniformly pick points on sphere for rand direction
T=2*pi*rand;F=asin(-1+2*rand);  % distributions for Theta & Phi
[rX, rY, rZ]=sph2cart(T,F,1);   % translate to Cartesian coord
random_dir=[rX rY rZ];          % random direction
coeff=sqrt(6*D*dt);             % new var for Brownian force
```

```
12 force_external_contrib=(1/zeta)*(-beta.*drift.*dt); % external
13 force_Brownian_contrib=coeff*random_dir;     % Brownian
14 displacement=force_external_contrib + force_Brownian_contrib;% total
15 centers(j+1,:)=centers(j,:)+ displacement;   % new position
```

First, the diffusion is calculated (line 1) as seen in section 2.2.2. From there, ζ is calculated (line 2). Next, the drift is calculated as in section 2.2.1 (lines 4-6). In lines 7-10, we see our uniform distributions for choosing angles for a segment of a sphere in order to choose a direction for the Brownian displacement. Line 11 calculates the magnitude of the Brownian displacement, as found in 2.2.2. The displacement that occurs due to each force is calculated in lines 12-13, and the total in line 14. The particle moves according to the calculated displacement in line 15. This is the first guess at the particle's new position before checking to see if the particle is within the boundary of the channel walls or has exited from either end of the channel.

2.3 Boundary of the channel

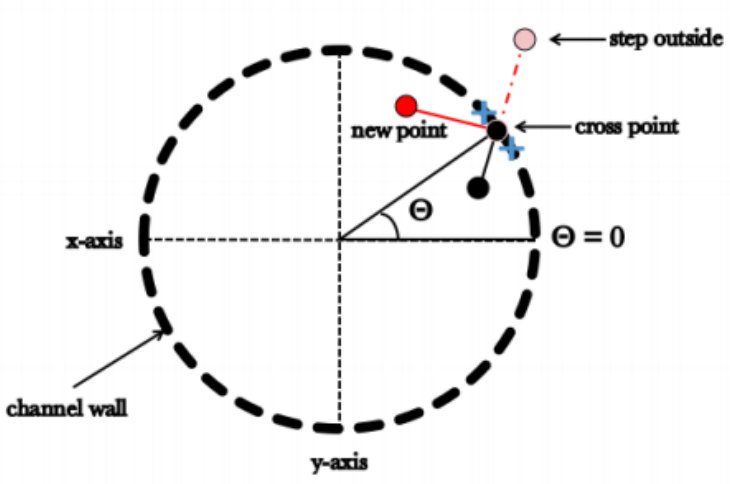

Figure 7: Illustration of boundary reflection

Actual particles cannot diffuse through the walls of the central channel, but must exit out of the nuclear or cytoplasmic end. To simulate this behavior, when the model particle attempts to pass through the wall, the point at which the edge of the particle would hit the channel wall if it were to move to its next position is approximated (called "crossPt" in the following sample of code). It will then be reflected away from the wall towards the center of the channel using the normal vector at the particle's position (called "NormalVector"). The normal vector is rotated (line 8) by the angle, θ (line 6), where the crossPt is located from the x-axis (see Figure 7). The trajectory that the particle would follow to the position that is outside of the cylinder is decomposed to create a new trajectory from the crossPt (to mimic a reflection) to a new location inside of the cylinder (lines 10-22). The magnitude of the distance the particle moves from the crossPt to the new position will be equal to the magnitude from the crossPt to the position that was outside of the cylinder. Below is an excerpt from the main script (which does not need to be edited by the user) to showcase how the boundary reflections are handled.

```
1  % If the edge of the particle lays outside of the cylinder,
2  % rotate about the z axis to move inside
3  while cyl_radius<edgeDist_next
4      % Find theta angle from crossing point
5      arccosX=acos(crossPt(1)/sqrt(crossPt(1)^2+crossPt(2)^2));
6      theta=sign(crossPt(2))*arccosX; % use y sign for theta sign
7      % Rotate the normal vector by theta
8      RotatedNormal=(1/norm(NormalVector))*[-cos(theta)...
9                                  -sin(theta) fp_value];
10     % Decomposition of vectors
11     bad_out_traj=next-crossPt;      % part we want to decompose
12     % parallel portion of bad trajectory
13     bad_out_trajPara=dot(bad_out_traj,RotatedNormal)*RotatedNormal;
14     % perpendicular portion of bad trajectory
```

```
15      bad_out_trajPerp=bad_out_traj-bad_out_trajPara;
16      % change sign of parallel portion of bad trajectory
17      good_out_trajPara=-bad_out_trajPara;
18      % keep old perpendicular portion
19      good_out_trajPerp=bad_out_trajPerp;
20      % create new vector
21      good_out_traj=good_out_trajPara+good_out_trajPerp;
22      % New point that will be inside the boundary
23      new_edgeloc=good_out_traj+crossPt;
24  end
25  % Update particle's position from first guess
26  new_center_pos=new_edgeloc-r*displacement_normd;
27  centers(j+1,:)=new_center_pos;
```

2.4 Calculating efficiencies

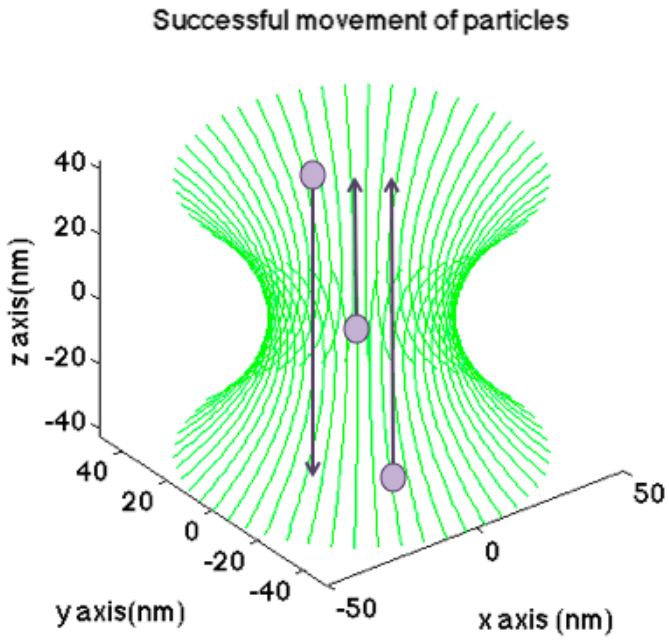

Particles that start in the center of the channel or on the nuclear side of the channel and then exit out of the cytoplasmic end of the channel are considered to be “exporting,” and the

efficiencies calculated are called *export* efficiencies. Particles that begin at the cytoplasmic end of the channel and exit out of the nuclear side are considered to be "importing," and the efficiencies of these particles are called *import* efficiencies. The results of this simulation will be given in terms of export efficiencies.

CHAPTER 3

RESULTS

Export efficiencies for the simulated particles are shown in Table (3). Simulations were run 600 times for each energy and starting position. Errors were calculated with a 90% confidence interval. When the particle began in the center of the channel with a constant PE, it had a, $\sim 50\%$ export efficiency rate, which makes sense due to the particle's diffusion only being affected by the random, or Brownian, force. Also, when there was a constant PE, if the particle began on either side of the central channel, it was less likely that it would travel to the opposite end. When there was a positive linear PE throughout the channel, the particles were unable to export from the channel unless they began very close to the cytoplasm, and even then, there was only $\sim 10\%$ efficiency. We see the opposite happens, which is what we would expect, when a negative linear PE is present. If the particle starts a greater distance away from the cytoplasm, its efficiency is affected, but it will still be greater than 80%. When there is a negative quadratic PE present in the channel, if the particle starts in the center of the channel, it will have $\sim 50\%$ export efficiency. However, if that particle is near the nuclear, it will not be able to overcome the drift to export to the cytoplasm. The hyperbolic tangent PE is interesting: no matter where the particle starts, there is some chance (however unlikely) for it to export to the cytoplasm. It seems as this function can be manipulated to see what parameters can increase the efficiency when the particle starts at the center or nucleus side of the channel.

The slope of the PE functions will be affected by the size of the particle, type of particle and its cargo, and also different levels of importin-β and crm1 that is available. For small particles, experimental results from Table (1) showed a $\sim 50\%$ efficiency for exporting and that efficiency seemed to increase for larger particles. For our model, the constant PE function represented the case of small particles and outputted the same $\sim 50\%$ export efficiency. If we take a closer look at the linear PE function (for example, the positively-

sloped PE), we can see how the amount of available kaps change the efficiency for larger particles. The slope is proportional to the amount of importin-β available in the nucleus (positive linear PE) or to the amount of crm1 available in the cytoplasm (negatively linear PE). Table (4) shows various instances of available importin-β in the nucleus. When there is a higher magnitude (more kaps), we see a higher import efficiency. When the slope lowers (less kaps), the import efficiency does, as well. A similar instance occurs when we explore different amplitudes of the hyperbolic tangent PE (Table 5).

		Initial Position	
Potential Energy	**Center**	**Negative/Nucleus**	**Positive/Cytoplasm**
Constant	$51.17 \pm 2.35\%$	$6.5 \pm 1.60\%$	$90.67 \pm 0.47\%$
Pos. Linear	$0 \pm 0\%$	$0 \pm 0\%$	$10.67 \pm 1.96\%$
Neg. Linear	$100 \pm 0\%$	$89.33 \pm 0.68\%$	$100 \pm 0\%$
Neg. Quadratic	$52.33 \pm 2.32\%$	$0 \pm 0\%$	$100 \pm 0\%$
Hyp. Tangent	$2.33 \pm 1.00\%$	$5.0 \pm 1.43\%$	$93.5 \pm 0.42\%$

Table 3: Export efficiencies found numerically

PE function	**Export Efficiency**	**Import Efficiency**	**ΔE (kT)**
$E(z) = 2 \cdot .001z$	0%	100%	1
$E(z) = 1 \cdot .001z$	0%	100%	0.5
$E(z) = .5 \cdot .001z$	1%	99%	0.25
$E(z) = .25 \cdot .001z$	8.8%	91.2%	0.125
$E(z) = .125 \cdot .001z$	25.3%	74.7%	0.0625
$E(z) = .0625 \cdot .001z$	35.8%	64.2%	0.0312
$E(z) = .0312 \cdot .001z$	47.2%	52.8%	0.0156

Table 4: Efficiencies for positive linear PE functions for particles beginning in the center of the NPC

PE function	Export Efficiency	Import Efficiency	ΔE (kT)
$E(z) = 2 \cdot .001 \tanh 5z$	0%	100%	1
$E(z) = 1 \cdot .001 \tanh 5z$	2.3%	97.7%	0.5
$E(z) = .5 \cdot .001 \tanh 5z$	18.5%	81.5%	0.25
$E(z) = .25 \cdot .001 \tanh 5z$	33.6%	66.4%	0.125
$E(z) = .125 \cdot .001 \tanh 5z$	43.8%	56.2%	0.0625
$E(z) = .0625 \cdot .001 \tanh 5z$	44.2%	55.8%	0.0312
$E(z) = .0312 \cdot .001 \tanh 5z$	48.2%	51.8%	0.0156

Table 5: Efficiencies for hyperbolic tangent PE functions for particles beginning in the center of the NPC

PE Function	Export Efficiency (%)	ΔE (kT)
$E(z) = 16 \cdot .001 \tanh 5(z+0.5)$	19.2	8
$E(z) = 8 \cdot .001 \tanh 5(z+0.5)$	28.5	4
$E(z) = 4 \cdot .001 \tanh 5(z+0.5)$	35.1	2
$E(z) = 2 \cdot .001 \tanh 5(z+0.5)$	40.5	1
$E(z) = 1 \cdot .001 \tanh 5(z+0.5)$	42.3	0.5
$E(z) = .5 \cdot .001 \tanh 5(z+0.5)$	46.8	0.25
$E(z) = .25 \cdot .001 \tanh 5(z+0.5)$	48.7	0.125

Table 6: Export efficiencies for shifted hyperbolic tangent PE functions for particles beginning in the center of the NPC

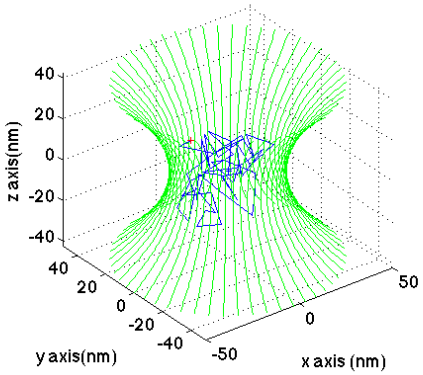

(a) $E(z) = .001$

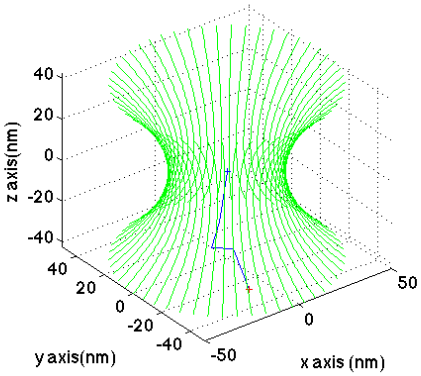

(b) $E(z) = .001z$

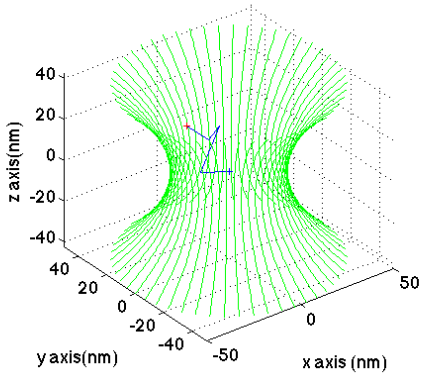

(c) $E(z) = -.001z$

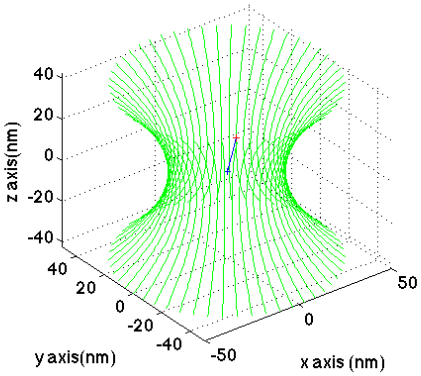

(d) $E(z) = -.001z^2$

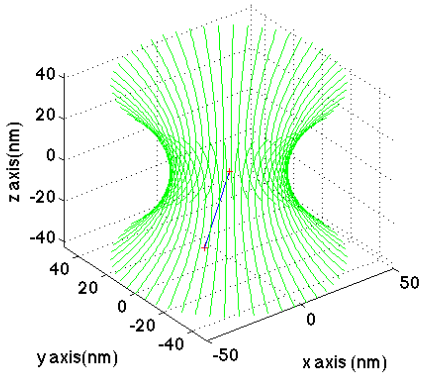

(e) $E(z) = .001 \tanh 5z$

Figure 8: Examples of particle transport when beginning in the center of the channel; when the particle exits (red marker) out of the positive end of the channel, it successfully exported, otherwise, it imported into the nucleus.

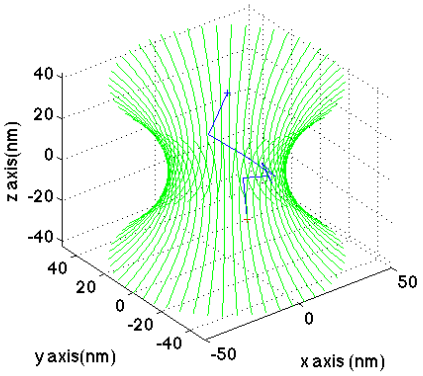

(a) Particle import with $E(z) = .001z$

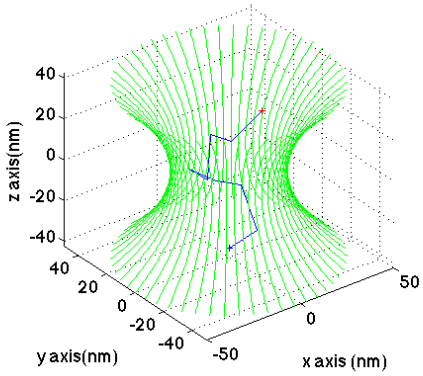

(b) Particle export with $E(z) = -.001z$

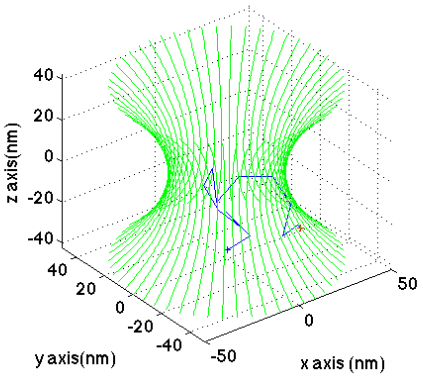

(c) Particle attempting to export, but insteads imports back to the nucleus with $E(z) = .001 \tanh 5z$

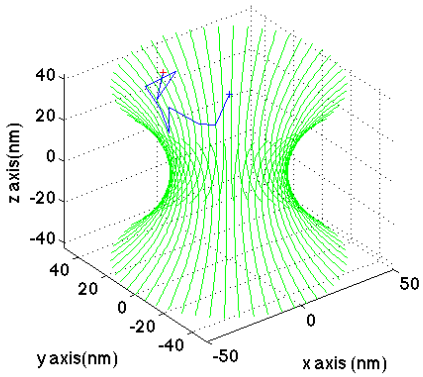

(d) Particle attempting to import, but insteads exports back to the cytoplasm with $E(z) = .001 \tanh 5z$

Figure 9: Additional examples of particle transport

CHAPTER 4

DISCUSSION

Our Langevin model uses Brownian dynamics to track the particle's position in three dimensions as it moves through the central channel of the NPC. If the channel was full of only fluid, the particles could be modeled solely by Brownian motion; however, due to the existence of FG repeats along the walls of the channel and kaps that must help larger particles, our model uses a PE function to mimic the drift and other influences on the particles. Because of the high density of FG repeats in the central channel, there is a large hydrophobic force attracting the particles [19].

Small particles that passively transport through the NPC do not need the help of kaps. They do not interact with the FG nups along the walls of the NPC and have no change in potential or binding energy. The constant PE function models this case, and our results of $\sim 50\%$ efficiency match experimental results (Table 1).

From the simulation data for the linear PEs, with a positive linear PE, the particle almost always returns to the nucleus and fails to export, while with a negative linear PE, the particle almost always exports to the cytoplasm. These energy functions may represent a combined effect of Ran-GTP/Ran-GDP concentration gradient across the NE and kaps involved in the import or export process. For nuclear import, importin-β assists cargo molecules in diffusing through the NPC and arrives to the nuclear side, where a high concentration of Ran-GTP in the nucleus dissociates the importin-β cargo complexes. Similarly, crm1 recognizes exporting cargo and assists them in diffusing through the NPC and then the complexes are dissociated by the Ran-GDP concentrated in the cytoplasm. This bidirectional transport process may be represented by the simulations under the positive or negative linear PE conditions. Additionally, the slope of the linear functions can further vary depending on the sizes of cargo molecules and the number of transport receptors clustered into the transitioning complexes. Originally, in the positive linear PE case, the PE

went from -0.25 kT to 0.25 kT, which seemed to give an optimal import efficiency. When this PE difference was increased twice as much (to go from -0.5 kT to 0.5 kT), we saw similar results. However, when the magnitude decreased, which caused the PE difference to decrease, the import efficiency dropped (see Table 4). This drop coincides with the kaps available in the nucleus to make their way into the pore to attach to cargo and aid them in transport. In the negative linear PE case, if the magnitude of the slope increases, the efficiency of exporting will be expected to decrease as well.

Additionally, the dense FG filaments in the center of the NPC make it difficult for the particles to organize in a way where they can pass through easily. For larger particles, this barrier causes higher entropy inside the pore. If there is an absence of kaps on either end of the NPC, the particles will have a difficult time transporting. The negative quadratic PE function simulates the high entropy that large particles must overcome in the center of the NPC due to the dense FG filaments when there is not enough available kaps. We see from the simulation results that without the chaperone of transport receptors, starting at either end of the NPC, the large particles are unable to import or export.

For a particle transporting with a positive linear PE, there was a very low chance of the particle exporting unless it started very close to the cytoplasmic wall (vise versa for importing with a negative linear function starting close to the nuclear face). We look at a similiar situation with the hyperbolic tangent energy function by "flattening" the slopes of the energy function towards each end of the NPC. Remarkably, the simulation data for the hyperbolic tangent PE function showed a much higher export efficiency (up to 94%) when particles begin at the cytoplasmic end of the NPC, but a small export efficiency elsewhere. This case is interpreted as representing a high concentration of Ran-GDP in the cytoplasm that will encourage export if near the cytoplasmic face. As in the linear PE case, the amplitude of this function can also vary and produce better or worse export/import efficiencies. Something to note about the hyperbolic tangent PE function is that when the function was shifted (Table 6), the export efficiency looked quite different. For a PE drop

of 1 kT, the export efficiency became 40.5%, compared to originally being 0% (Table 5).

In all of the cases of PE in Table (3), at the cytoplasmic end of the cylinder, the PE is roughly 0.25 kT, and at the nuclear end the PE is -0.25 kT. The change in PE across the cylinder then is 0.5 kT which makes up a portion of the binding energy the complex needs in order to travel across the NPC. In our calculation of ΔH (Equation 1), we attained a value of -0.85 kT for a transport receptor with a charge $-50e$. The value of ΔH will vary based on which transport receptor binds to the cargo and how many of them bind to the cargo due to the net charges associated with the receptors that attach; this will in turn, change how much energy the particle will need to be able to travel through the NPC. Both of the approximations, for ΔH and the PE are very simplistic and are just made to see the relationship of how they can vary in a similar way.

Overall, we were able to see how the change in PE throughout the system affected the import and export efficiency for particles transporting through the NPC. We were interested in understanding which factors influence the success and/or failure of the particle transport and which of those can be manipulated to cause a change in the import and export efficiencies. With this proposed (and easily adjusted) model, we were able to study five different scenarios that take place in the NPC and how factors such as the curvature of the channel and the concentration of the kaps within the NPC affect the import and export of particles. More simulations can be run to study the differences between a linear energy function to represent changes in the concentrations of a particular transport receptor. Further studies can explore variations in the hyperbolic tangent energy function to see changes in efficiency depending on the "flattened" slope on the outer ends of the NPC representing different levels of Ran-GTP/GDP encouraging import/export. Of course, different curvatures could also be tested to see if the geometry of the channel plays a large role in import/export efficiency; from this, we can gain a deeper understanding of the reason for the shape the NPC naturally holds. This 3D simulation serves as an easy to use basis and beginning model for further research and exploration.

REFERENCES

[1] Berg, H. C. (Expanded Ed.) (1993). Random walks in biology. Princeton University Press.

[2] Bressloff, P. C., & Newby, J. M. (2013). Stochastic models of intracellular transport. *Reviews of Modern Physics*, 85(1), 135.

[3] Brown, R. (1828). A Brief Account of Microscopical Observations Made... on the Particles Contained in the Pollen of Plants, and on the General Existence of Active Molecules in Organic and Inorganic Bodies.

[4] Colwell, L. J., Brenner, M. P., Ribbeck, K., & Gilson, M. (2010). Charge as a selection criterion for translocation through the nuclear pore complex. *PLoS Comput Biol*, 6(4), e1000747-e1000747.

[5] Cooper, G.M. (2000). The Nuclear Envelope and Traffic between the Nucleus and Cytoplasm. *The Cell: A Molecular Approach. 2nd edition*. Sunderland (MA): Sinauer Associates.

[6] Doob, J. L. (1942). The Brownian movement and stochastic equations. *Annals of Mathematics*, 351-369.

[7] Einstein, A. (1956). Investigations on the Theory of the Brownian Movement. Courier Corporation.

[8] Giancoli, D. C. (2005). *Physics: principles with applications*. Pearson Education.

[9] Hoelz, A., Debler, E. W., & Blobel, G. (2011). The structure of the nuclear pore complex. *Annual review of biochemistry*, 80, 613-643.

[10] Macara, I. G. (2001). Transport into and out of the nucleus. *Microbiology and Molecular Biology Reviews*, 65(4), 570-594. Chicago

[11] Ma, J., Liu, Z., Michelotti, N., Pitchiaya, S., Veerapaneni, R., Androsavich, J. R., ... & Yang, W. (2013). High-resolution three-dimensional mapping of mRNA export through the nuclear pore. *Nature communications*, 4.

[12] Ma, J., Goryaynov, A., Sarma, A., & Yang, W. (2012). Self-regulated viscous channel in the nuclear pore complex. *Proceedings of the National Academy of Sciences*, 109(19), 7326-7331.

[13] Mainardi, F., & Pironi, P. (2008). The fractional Langevin equation: Brownian motion revisited. *arXiv preprint* arXiv:0806.1010.

[14] Margulis, L., Dolan, M. F., & Guerrero, R. (2000). The chimeric eukaryote: Origin of the nucleus from the karyomastigont in amitochondriate protists. *Proceedings of the National Academy of Sciences of the United States of America*, 97(13), 69546959.

[15] Mohr, D., Frey, S., Fischer, T., Güttler, T., & Görlich, D. (2009). Characterisation of the passive permeability barrier of nuclear pore complexes. *The EMBO journal*, 28(17), 2541-2553.

[16] Mogilner, A., Elston, T. C., Wang, H., & Oster, G. (2002). Molecular motors: theory. In *Computational cell biology* (pp. 320-353). Springer New York.

[17] Mood, A.M., Graybill, F.A. & Boes, D.C. (1974) (3rd Ed.) Introduction to the theory of statistics. McGraw-Hill Kokagusha.

[18] Moussavi-Baygi, R., Jamali, Y., Karimi, R., & Mofrad, M. R. (2011). Brownian dynamics simulation of nucleocytoplasmic transport: a coarse-grained model for the functional state of the nuclear pore complex. *PLoS computational biology*, 7(6), e1002049.

[19] Moussavi-Baygi, R., Jamali, Y., Karimi, R., & Mofrad, M. R. K. (2011). Biophysical coarse-grained modeling provides insights into transport through the nuclear pore complex. *Biophysical journal*, 100(6), 1410-1419.

[20] Nelson, E. (1967). Dynamical theories of Brownian motion (Vol. 17). *Princeton: Princeton university press*.

[21] Schoch, R. L., Kapinos, L. E., & Lim, R. Y. (2012). Nuclear transport receptor binding avidity triggers a self-healing collapse transition in FG-nucleoporin molecular brushes. *Proceedings of the National Academy of Sciences*, 109(42), 16911-16916.

[22] Suntharalingam, M., & Wente, S. R. (2003). Peering through the pore: nuclear pore complex structure, assembly, and function. *Developmental cell*, 4(6), 775-789.

[23] Tran, E. J., & Wente, S. R. (2006). Dynamic nuclear pore complexes: life on the edge. *Cell*, 125(6), 1041-1053.

[24] Tu, Li-Chun, Fu, G., Zilman, A., & Musser, S. M. (2013). Large cargo transport by nuclear pores: implications for the spatial organization of FG-nucleoporins. *The EMBO Journal*, uncorrected proof.

[25] Wente, S. R., & Rout, M. P. (2010). The nuclear pore complex and nuclear transport. *Cold Spring Harbor perspectives in biology*, 2(10), a000562.